Characterization of Vanadium Oxide Supported on Zirconia and Modified with MoO_3

Jong Rack Sohn,* Ki Cheol Seo, and Young Il Pae†

Dept. of Industrial Chemistry, Engineering College, Kyungpook National University, Daegu 702-701, Korea
†Dept. of Chemistry, University of Ulsan, Ulsan 680-749, Korea
Received July 19, 2002

Vanadium oxides supported on zirconia and modified with MoO_3 were prepared by adding $Zr(OH)_4$ powder into a mixed aqueous solution of ammonium metavanadate and ammonium molybdate followed by drying and calcining at high temperatures. The characterization of prepared catalysts was performed using FTIR, Raman spectroscopy and solid-state ^{51}V NMR. In the case of a calcination temperature of 773 K, for samples containing low loading of V_2O_5, below 15 wt %, vanadium oxide was in a highly dispersed state, while for samples containing high loading of V_2O_5, equal to or above 15 wt %, vanadium oxide was well crystallized because the V_2O_5 loading exceeded the formation of a monolayer on the surface of ZrO_2. The ZrV_2O-compound was formed through the reaction of V_2O_5 and ZrO_2 at 873 K and the compound decomposed into V_2O_5 and ZrO_2 at 1073 K, which were confirmed by FTIR spectroscopy and solid-state ^{51}V NMR. IR spectroscopic studies of ammonia adsorbed on V_2O_5-MoO_3/ZrO_2 showed the presence of both Lewis and Brönsted acids.

Key Words : Characterization, V_2O_5-MoO_3/ZrO_2, ^{51}V NMR, FTIR, XRD

Introduction

Vanadium oxides are widely used as catalysts in oxidation reactions, for example, the oxidation of sulfur dioxide, carbon monoxide, and hydrocarbons.[1-4] These systems have also been found to be effective catalysts for the oxidation of methanol to methylformate[5,6] and for the ammoxidation of 3-picoline.[7] Vanadia catalysts supported on titania-alumina mixed oxide and titania modified with alumina were found to exhibit superior activities in selective catalytic reduction of NOx.[8-11] Much research has been done to understand the nature of active sites, the surface structure of catalysts as well as the role played by the promoter of the supported catalysts, using infrared (IR), X-ray diffraction (XRD), electron spin resonance (E.S.R) and Raman spectroscopy.[12-14] So far, silica, titania, zirconia and alumina[15-21] have been commonly employed as the vanadium oxide supports.

Recently, metal oxides modified with sulfur compounds have been studied as strong solid acidic catalysts,[22-24] especially sulfate promoted zirconia containing iron or manganese as promoters[25,26] or noble metals to inhibit deactivation.[27,28] The high catalytic activity and small deactivation upon the addition of noble metals can be explained by both the elimination of coke by hydrogenation and hydrogenolysis.[29] and the formation of Brönsted acid sites from H_2 on the catalysts.[28] Recently, Zhao et al. reported zirconia-supported molybdenum oxide as an alternative material for reactions requiring strong acid sites.[30] Several advantages of molybdate, over sulfate, as dopant include that it does not suffer from dopant loss during thermal treatment and it undergoes significantly less deactivation during catalytic reactions.[31] So far, however, comparatively few studies have been reported on binary oxide, vanadium oxide-molybdenum oxide supported on zirconia.

It is well known that the dispersion and the structural features of supported species are strongly dependent on the support. The promoting effect of a TiO_2 support on the oxidation of o-xylene on V_2O_5 has been ascribed to an increase of the number of surface V=O bonds on the V_2O_5/TiO_2 catalysts and weakening of these bonds.[32] In many studies concerning the mechanism of the catalytic reactions on vanadium oxide, the V=O species have been considered to play a significant role as the active sites for the reactions.[33] Structure and other physicochemical properties of supported metal oxides are considered to be in different states compared with bulk metal oxides because of their interaction with the supports. Solid-state nuclear magnetic resonance (NMR) methods represent a novel and promising approach to these systems. Since only the local environment of a nucleus under study is probed by NMR, this method is well suited for the structural analysis of disordered systems such as the two-dimensional surface vanadium oxide phases which is of particular interest in the present study. In addition to the structural information provided by NMR methods, the direct proportionality of the signal intensity to the number of contributing nuclei makes NMR be useful for quantitative studies. In the present investigation, the techniques of solid-state ^{51}V NMR and Fourier transform infrared (FTIR) have been utilized to characterize a series of V_2O_5 samples supported on ZrO_2 and modified with MoO_3.

Experimental Section

Catalyst Preparation. Precipitate of $Zr(OH)_4$ was obtained by adding aqueous ammonia slowly into an aqueous solution of zirconium oxychloride (Aldrich) at room temperature

*Corresponding author. E-mail: jrsohn@knu.ac.kr

with stirring until the pH of mother liquor reached about 8. The precipitate thus obtained was washed thoroughly with distilled water until chloride ion was not detected by $AgNO_3$ solution, and was dried at room temperature for 12 h. The dried precipitate was powdered below 100 mesh.

The catalysts containing various vanadium oxide content and modified with MoO_3 were prepared by adding $Zr(OH)_4$ powder into a mixed aqueous solution of ammonium metavanadate (NH_4VO_3) (Aldrich) and ammonium molybdate $[(NH_4)_6(Mo_7O_{24})(4H_2O)$ (Aldrich) followed by drying and calcining at high temperatures for 1.5 h. This series of catalysts were denoted by their weight percentage of V_2O_5 and MoO_3 and calcination temperature. For example, $3V_2O_5$-$15MoO_3/ZrO_2(773)$ indicated the catalyst containing 3 wt% V_2O_5 and 15 wt% MoO_3 calcined at 773 K.

Characterization. FTIR absorption spectra of V_2O_5-MoO_3/ZrO_2 powders were measured by KBr disk method over the range 1200-400 cm^{-1}. The samples for the KBr disk method were prepared by grinding a mixture of the catalyst and KBr powders in an agate mortar and pressing them in the usual way. FTIR spectra of ammonia adsorbed on the catalyst were obtained in a heatable gas cell at room temperature using a Mattson Model GL 6030E spectrophotometer. The self-supporting catalyst wafers contained about 9 mg/cm^2. Before the spectra were obtained, the samples were heated under vacuum at 673-773 K for 1.5 h.

The FT-Raman spectra were obtained with a Bruker model FRA 106 A spectrometer equipped with an InGaAs detector and a Nd:YAG laser source with a resolution of 4 cm^{-1}. The laser beam was focussed onto an area 0.1×0.1 mm^2 in size of the sample surface; a 180° scattering geometry was used.

^{51}V NMR spectra were measured by a Varian Unity Inova 300 spectrometer with a static magnetic field strength of 7.05 T. Larmor frequency was 78.89 MHz. An ordinary single pulse sequence was used, in which the pulse width was set at 2.8 s and the acquisition time was 0.026 s. The spectral width was 500 kHz. The number of scans was varied from 400 to 4,000, depending on the concentration of vanadium. The signal was acquired from the time point 4 s after the end of the pulse. The sample was static, and its temperature was ambient (294 K). The spectra were expressed with the signal of $VOCl_3$ being 0 ppm, and the higher frequency shift from the standard was positive. Practically, solid NH_4VO_3 (-571.5 ppm) was used as the second external reference.[34-36]

Results and Discussion

Infrared Spectra. Figure 1 shows IR spectra of V_2O_5-$15MoO_3/ZrO_2(773)$ catalysts with various V_2O_5 contents calcined at 773 K for 1.5 h. Although with samples having less than 18 wt % of V_2O_5 definite peaks were not observed, the absorption bands at 1022 and 818 cm^{-1} appeared for $15V_2O_5$-$15MoO_3/ZrO_2$, $20V_2O_5$-$15MoO_3/ZrO_2$, $25V_2O_5$-$15MoO_3/ZrO_2$ and pure V_2O_5 containing high V_2O_5 content. The band at 1022 cm^{-1} was assigned to the V=O stretching vibration, while that at 818 cm^{-1} was attributable to the coupled vibration between V=O and to V-O-V.[36,37] Generally, the IR band of V=O in crystalline V_2O_5 showed at 1020-1025 cm^{-1} and the Raman band at 995 cm^{-1}.[2,38] The intensity of the V=O absorption gradually decreased with increasing ZrO_2 content, although the band position did not change. This observation suggests that vanadium oxide below 15 wt % is in a highly dispersed state. It is reported that V_2O_5 loading exceeding the formation of monolayer on the surface of ZrO_2 is well crystallized and observed in the spectra of IR and solid state ^{51}V NMR.[34,36]

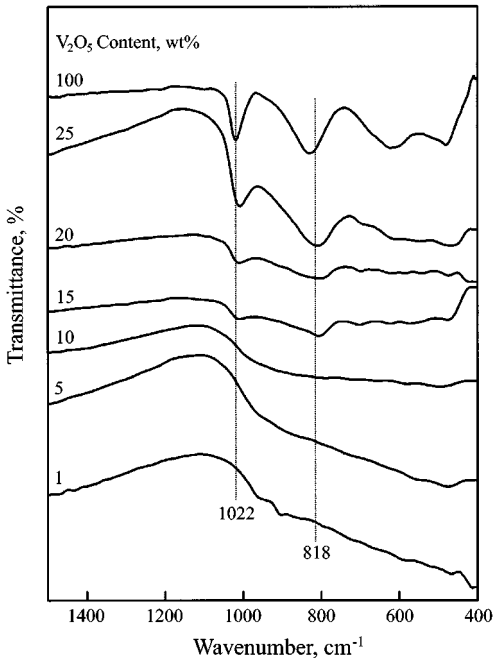

Figure 1. Infrared spectra of V_2O_5-$15MoO_3/ZrO_2$ (773) catalysts with different V_2O_5 contents.

It is necessary to examine the formation of crystalline V_2O_5 as a function of calcination temperature. Variation of IR spectra against calcination temperature for $3V_2O_5$-$15MoO_3/ZrO_2$ is shown in Figure 2. There were no V=O stretching bands at 1022 cm^{-1} at calcination temperatures from 673 to 973 K, indicating no formation of crystalline V_2O_5. However, as shown in Figure 2, V=O stretching bands due to crystalline V_2O_5 at 1073 and 1173 K appeared at 1022 cm^{-1} together with lattice vibration bands of V_2O_5 and MoO_3 below 900 cm^{-1}.[35,39] The formation of crystalline V_2O_5 at above 1073 K can be explained in terms of the decomposition of ZrV_2O_7 compound which was formed through the reaction of V_2O_5 and ZrO_2 at 873-973 K. In this study, on X-ray diffraction patterns the cubic phase of ZrV_2O_7 was observed in the samples calcined at 873 K and for sample calcined at 1173 K the ZrV_2O_7 phase disappeared due to the decomposition of ZrV_2O_7, leaving the V_2O_5 phase and the monoclinic phase of ZrO_2. These results are in good agreement with those of ^{51}V solid state NMR described later. In fact, it is known that the formation of ZrV_2O_7 from V_2O_5 and ZrO_2 occurs at calcination temperature of 873 K and the ZrV_2O_7 decomposes into ZrO_2 and V_2O_5 at 1073 K.[34,36,40] In separate experiments, variation of IR spectra against calcination temperature for $10V_2O_5$-$15MoO_3/ZrO_2$ (not shown in the Figure) was similar

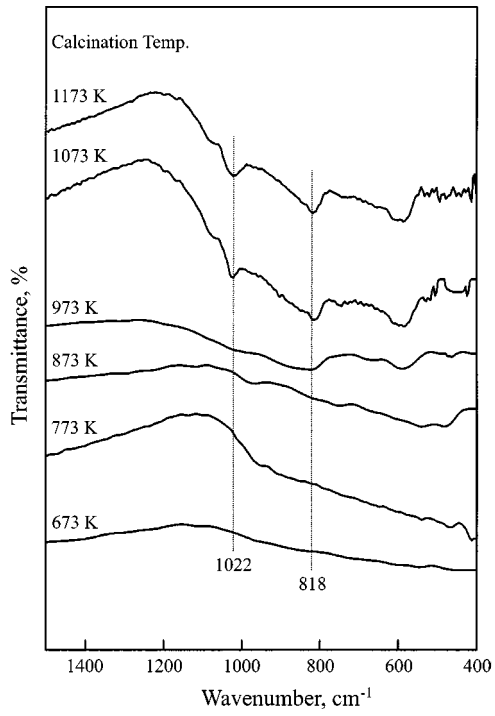

Figure 2. Infrared spectra of $3V_2O_5$-$15MoO_3/ZrO_2$ catalysts calcined at different temperatures.

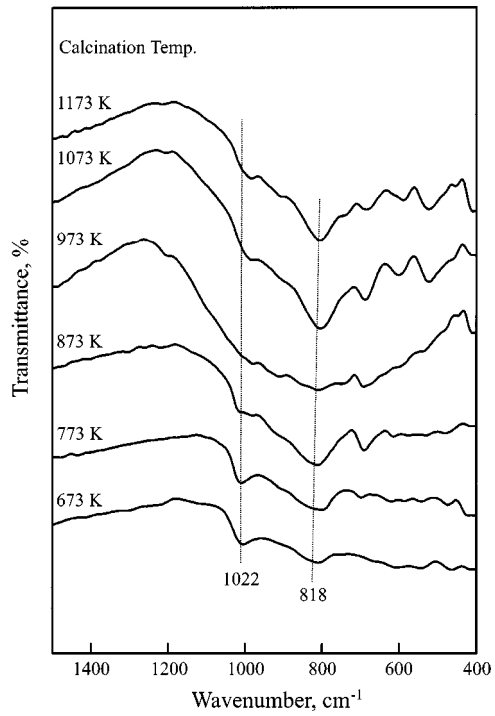

Figure 3. Infrared spectra of $20V_2O_5$-$15MoO_3/ZrO_2$ catalysts calcined at different temperatures.

to that for $3V_2O_5$-$15MoO_3/ZrO_2$ as shown in Figure 2.

Figure 3 shows IR spectra of $20V_2O_5$-$15MoO_3/ZrO_2$ catalysts calcined at 673-1173 K for 1.5h. Unlike $3V_2O_5$-$15MoO_3/ZrO_2$ and $10V_2O_5$-$5MoO_3/ZrO_2$ catalysts, for $25V_2O_5$-$15MoO_3/ZrO_2$ crystalline V_2O_5 appeared at a lower calcination temperature from 673 K to 873 K and consequently V=O

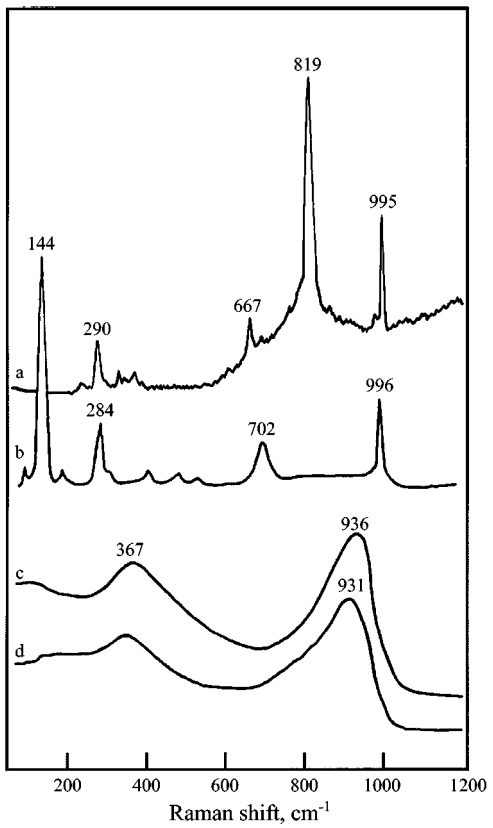

Figure 4. Raman spectra of (a) MoO_3, (b) V_2O_5, (c) $10V_2O_5$-$15MoO_3/ZrO_2$(773), and (d)$15V_2O_5$-$15MoO_3/ZrO_2$(773).

stretching band was observed at 1022 cm^{-1}. This is because a V_2O_5 loading exceeding the formation of monolayer on the surface of ZrO_2 is well crystallized.[34] However, at 973 K all V_2O_5 reacted with ZrO_2 and changed into ZrV_2O- so that V=O stretching at 1022 cm^{-1} disappeared completely, as shown in Figure 3.

At a calcination temperature of 1073 K, some of the ZrV_2O- decomposed into V_2O_5 and ZrO_2 and then V=O stretching band due to the crystalline V_2O_5 was again observed at 1022 cm^{-1}. These are in good agreement with those of ^{51}V solid-state NMR described later

Raman spectra. Raman spectroscopy is a valuable tool for the characterization of dispersed metal oxides and detects vibrational modes surface and bulk structures. In order to analyze the nature of the surface species, laser Raman measurements of bulk MoO_3, bulk V_2O_5 and V_2O_5-$15MoO_3/ZrO_2$ samples calcined at 773 K and with different vanadium oxide loadings were made. Figure 4 shows Raman spectra of four samples under ambient condition. Bulk MoO_3, obtained by calcining ammonium molybdate at 773 K, shows the main bands in good agreement with data previously reported.[41,42] The major vibrational modes of MoO_3 [Figure 4(a)] are located at 995, 819,667 and 290 cm^{-1}, and have been assigned to the Mo=O stretching mode, the Mo-O-Mo asymmetric stretching mode, the Mo-O-Mo symmetric stretching mode, and the M=O bending mode, respectively.[41,42]

We will discuss the Raman spectrum of the bulk V_2O_5, obtained by calcining ammonium metavanadate at 773 K,

which is shown in Figure 4(b). The spectrum displayed bands at 144, 196, 284, 304, 406, 484, 528, 702 and 996 cm^{-1}, all of which are characteristic of crystalline V_2O_5.[43] The 996 cm^{-1} band is assigned to the vibration of the short vanadium oxygen bond normally regarded as a V=O species.[43] However, as shown in Figure 4(c), for $10V_2O_5$-$15MoO_3/ZrO_2$ (773) no bands corresponding to MoO_3 and V_2O_5 crystallites appear, indicating that MoO_3 and V_2O_5 are in a highly dispersed state. As described in IR spectra, the catalysts at vanadia loadings below 15 wt% gave no absorption bands due to crystalline V_2O_5. However, as shown in Figure 4(d), for $15V_2O_5$-$15MoO_3/ZrO_2$(773) containing 15% V_2O_5 the bands due to V_2O_5 crystalline were observed, showing good agreement with the results of IR spectra.

The molecular structure of the supported molybdenum oxide species depends on the loading. Several authors observed that the nature of surface molybdenum species on SiO_2, Al_2O_3, TiO_2 and ZrO_2 depends on the amount of MoO_3. Raman bands between 910 and 980 cm^{-1} are usually attributed to the Mo=O vibration of Mo species in either octahedral or tetrahedral environment.[44] Generally, monomolybdate or tetrahedral molybdenum oxygen species have been assigned for low MoO_3 loading samples.[42,44,45] and two-dimensional polymolybdates or octahedral molybdenum-oxygen species with characteristic band around 950-980 cm^{-1}, for high MoO_3 loading samples.[42,44,45] The frequency of Raman feature (1000-940 cm^{-1}), the maximum of which shifts slightly upwards on increasing vanadium content, is assigned to the V=O stretching mode vanadyl species in a hydrated form.[9,46] Therefore, the broad band observed in the 950-1000 cm^{-1} region in Figure 4(c and d) will be interpreted as an overlap of three characteristic bands(two molybdenum oxide species and one vanadyl species).

For $10V_2O_5$-$15MoO_3$/ ZrO_2(773) and $15V_2O_5$-$15MoO_3$/ ZrO_2(773) in Figure 4(c and d), most of zirconia is amorphous to x-ray diffraction, showing tiny amount of tetragonal phase zirconia. The Raman spectrum of amorphous zirconia is characterized by a very weak and broad band at 550-600 cm^{-1}.[47] Tetragonal zirconia is expected to yield a spectrum consisting of Raman bands in the region of 150-640 cm^{-1}.[36,48] Therefore the very broad band around 367 cm^{-1} is interpreted as an overlap of amorphous and tetragonal phase zirconia.

Solid-State ^{51}V NMR Spectra. Solid-state NMR methods represent a promising approach to vanadium oxide catalytic materials. The solid state ^{51}V NMR spectra of V_2O_5-MoO_3/ ZrO_2 catalysts calcined at 773 K followed by exposure to air are shown in Figure 5. There are three types of signals in the spectra of catalysts with varying intensities depending on V_2O_5 content. At low loadings up to 10 wt% V_2O_5 a shoulder at about -260 ppm and an intense peak at -590~-650 ppm are observed. The former is assigned to the surface vanadium-oxygen structures surrounded by a distorted octahedron of oxygen atoms, while the latter is attributed to the tetrahedral vanadium-oxygen structures.[49,50]

However, the surface vanadium oxide structure is remarkably dependent on the metal oxide support material. Vanadium

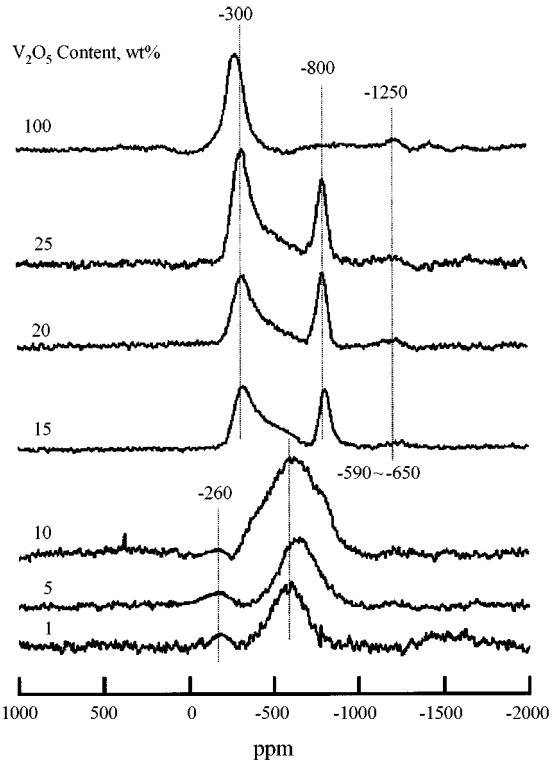

Figure 5. Solid-state ^{51}V NMR spectra of V_2O_5-$15MoO_3/ZrO_2$ (773) catalysts with different V_2O_5 contents.

oxide on TiO_2 (anatase) displays the highest tendency to be 6-coordinated at low surface coverages, while in the case of γ-Al_2O_3 a tetrahedral surface vanadium species is favored[50]. As shown in Figure 5, at a low vanadium loading on zirconia a tetrahedral vanadium species is exclusively dominant compared with a octahedral species. In general, it is known that low surface coverages favor a tetrahedral coordination of vanadium oxide, while at higher surface coverages vanadium oxide becomes increasingly octahedral-coordinated.

Increasing the V_2O_5 content on the zirconia surface changes the shape of the spectrum to a rather intense and sharp peak at about -300 ppm and a broad low-intensity peak at about -1250 ppm, which are due to the crystalline V_2O_5 of square pyramid coordination.[49] These observations of crystalline V_2O_5 for samples containing high V_2O_5 content, above 10 wt%, are in good agreement with the results of the IR spectra in Figure 1. Namely, this is because V_2O_5 loading exceeding the formation of monolayer on the surface of zirconia is well crystallized.[34-36] Moreover, the increase in V_2O_5 content resulted in the appearance of an additional signal with a peak at -800 ppm. The intensity of the signal increased with an increase in V_2O_5 loading. Different peak positions normally indicate the differences of the spectral parameters and are observed due to different local environments of vanadium nuclei.[49-53] Thus species at -500~-650 ppm and -800 ppm can be attributed to two types of tetrahedral vanadium complexes with different oxygen environments. Namely, the signals at -500~-650 ppm can be attributed to the surface vanadium complexes containing OH groups or water molecules in their coordination sphere.[50]

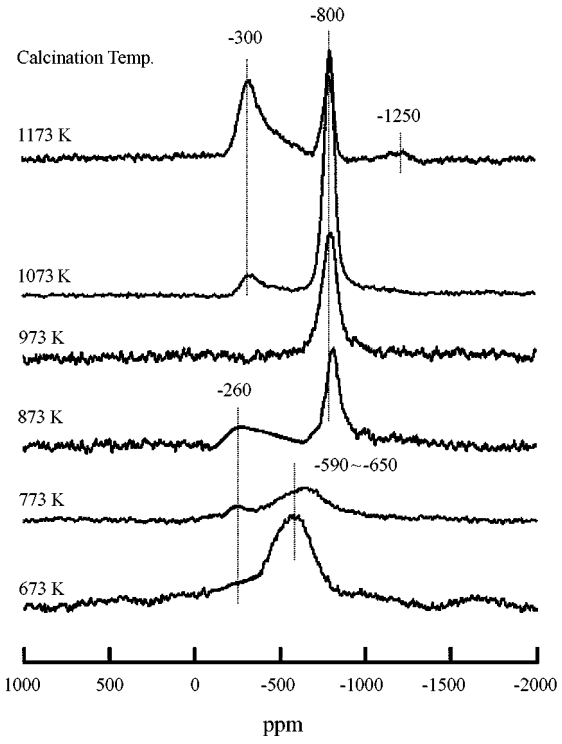

Figure 6. Soid-state ^{51}V NMR spectra of $3V_2O_5$-$15MoO_3/ZrO_2$ catalysts calcined at different temperatures.

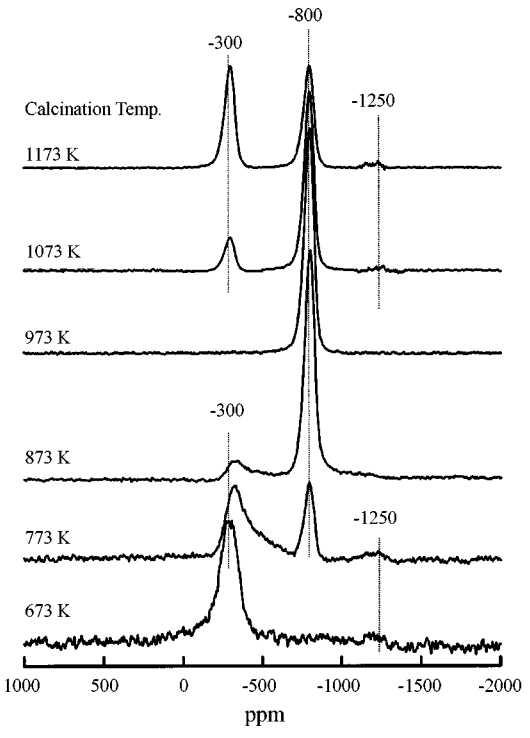

Figure 7. Solid-state ^{51}V NMR spectra of $20V_2O_5$-$15MoO_3$/ ZrO_2 catalysts calcined at different temperatures.

because the evacuation treatment decreases the intensities remarkably. On the other hand, the signal at -800 ppm is due to the surface tetrahedral vanadium complexe which does not contain OH groups or adsorbed water molecules.

It is necessary to examine the effect of calcination temperature on the surface of the vanadium oxide structure. The spectra of $3V_2O_5$-$15MoO_3/ZrO_2$ containing a lower vanadium oxide content and calcined at various temperatures are shown in Figure 6. The shape of the spectrum is very different depending on the calcination temperature. For both samples calcined at lower temperatures (673-773 K), two peaks at about -260 ppm and -500 ~ -650 ppm due to the octahedral and tetrahedral vanadium-oxygen structures are shown, indicating the monolayer dispersion of V_2O_5 on the ZrO_2 surface. These results are in good agreement with the results of the IR spectra in Figure 2. However, for samples calcined at 873 K, in addition to the above two peaks, a peak at -800 ppm due to crystalline ZrV_2O_7 appeared, indicating the formation of a new compound from V_2O_5 and ZrO_2 at a high calcination temperature. For samples calcined at 873-1073 K, X-ray diffraction patterns of ZrV_2O_7 were observed. Roozeboom *et al.* reported the formation of ZrV_2O_7 from V_2O_5 and ZrO_2 at a calcination temperature of 873 K.[40] At a calcination temperature of 973 K only a peak at -800 ppm due to the ZrV_2O_7 phase appeared, saying that most of the V_2O_5 on the surface of zirconia was consumed to form the ZrV_2O_7 compound. However, at a calcination temperature of 1073-1173 K we can observe only a sharp peak of crystalline V_2O_5 at -300 and about -1250 ppm, indicating the decomposition of ZrV_2O_7. These results are in good agreement with those of IR spectra in Figure 2.

The spectra of $20V_2O_5$-$15MoO_3/ZrO_2$ containing a higher vanadium oxide content than monolayer loading and calcined at various temperatures are shown in Figure 7. Unlike $3V_2O_5$-$15MoO_3/ZrO_2$, for $20V_2O_5$-$15MoO_3/ZrO_2$ calcined even at lower temperatures (773 K) a sharp peak due to crystalline V_2O_5 appeared at -300 ppm together with a peak at -800 ppm due to the tetrahedral surface species. However, for samples calcined at 873 K, in addition to a peak at -300 ppm due to crystalline V_2O_5, a sharp peak at -800 ppm due to ZrV_2O_7 compound appeared. As shown in Figure 7, the peak intensity of ZrV_2O_7 increased with an increase in calcination temperature, consuming the content of crystalline V_2O_5. Consequently, at a calcination temperature of 973 K only a peak due to the ZrV_2O_7 phase appeared at -800 ppm. At a calcination temperature of 1073 K, a sharp peak of crystalline V_2O_5 at -300 ppm due to the decomposition of ZrV_2O_7 was again observed. However, unlike $3V_2O_5$-$15MoO_3/ZrO_2$, for $20V_2O_5$-$15MoO_3/ZrO_2$, the ZrV_2O_7 compound was not decomposed completely at 1073 K, leaving some ZrV_2O_7. It seems likely that it is very difficult for all ZrV_2O_7 to decompose for 1.5 h because a large amount of ZrV_2O_7 was formed in the case of $20V_2O_5$-$15MoO_3/ZrO_2$.

Surface Properties. The specific surface areas of some samples calcined at 673 and 773 K for 1.5 h are listed in Table 1. The presence of vanadium oxide and molybdenum oxide influences the surface area in comparison with the pure ZrO_2. Specific surface areas of V_2O_5-MoO_3/ZrO_2 samples are larger than that of pure ZrO_2 calcined at the same temperature. It seems likely that the interaction between

Table 1. Specific surface areas of some V_2O_5-$15MoO_3/ZrO_2$ samples calcined at 673 K and 773 K

Catalysts	Surface area (m^2/g, 673 K)	Surface area (m^2 g, 773 K)
ZrO_2	185	122
$1V_2O_5$-$15MoO_3/ZrO_2$	219.9	218.6
$3V_2O_5$-$15MoO_3/ZrO_2$	236.2	221.4
$5V_2O_5$-$15MoO_3$ ZrO_2	223.8	216.8
$10V_2O_5$-$15MoO_3$ ZrO_2	207.9	165.6
$15V_2O_5$-$15MoO_3$ ZrO_2	170.1	148.6
$20V_2O_5$-$15MoO_3$ ZrO_2	164.5	147.1

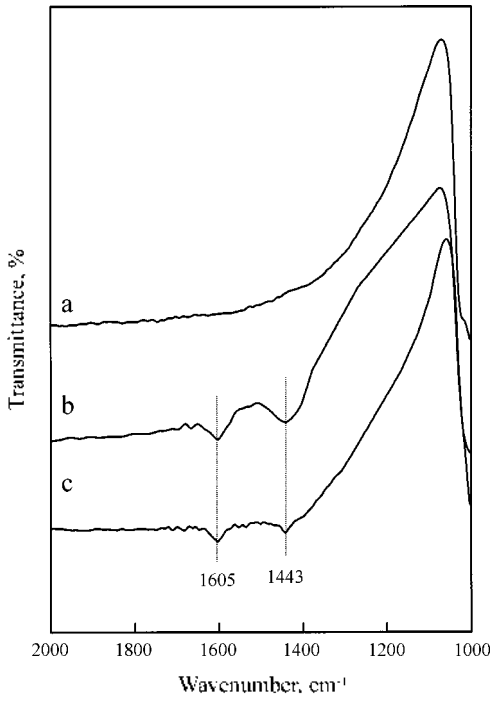

Figure 8. Infrared spectra of NH_3 adsorbed on $15V_2O_5$-$15MoO_3/ZrO_2$ (773). (a) background of $15V_2O_5$-$15MoO_3$ $/ZrO_2$ evacuated at 673 K for 1 h. (b) NH_3(20 torr) adsorbed on sample a, (c) sample b evacuated at 503 K for 0.5 h.

vanadium oxide (or molybdenum oxide) and ZrO_2 protects catalysts from sintering.[34]

Infrared spectroscopic studies of ammonia adsorbed on solid surfaces have made it possible to distinguish between Brönsted and Lewis acid sites.[23,54,55] Figure 8 shows the IR spectra of ammonia adsorbed on $15V_2O_5$-$15MoO_3/ZrO_2$ calcined at 773 K and evacuated at 673 K for 1 h. For $15V_2O_5$-$15MoO_3/ZrO_2$ the bands at 1443 are the characteristic peaks of ammonium ion, which are formed on the Brönsted acid sites and the absorption peaks at 1605 cm^{-1} are contributed by ammonia coordinately bonded to Lewis acid sites,[22,54] indicating the presence of both Brönsted and Lewis acid sites. Other samples having different vanadium content also showed the presence of both Lewis and Brönsted acids. Therefore, these V_2O_5-MoO_3/ZrO_2 samples can be used as catalysts for Lewis or Brönsted acid catalysis.

Conclusions

On the basis of the results of FTIR, Raman spectroscopy, solid-state ^{51}V NMR and XRD, at a low calcination temperature of 773 K, it has been found that vanadium oxide up to 10 wt% was well dispersed on the surface of zirconia. However, when the V_2O_5 loading exceeded 15 wt% (the amount equal to cover by monolayer on the surface of zirconia), the V_2O_5 existed in well crystallized state. The ZrV_2O- compound was formed by the reaction of V_2O_5 and ZrO_2 at 873 K and it decomposed into V_2O_5 and ZrO_2 at 1073 K; these results were observed in FTIR spectra and solid-state ^{51}V NMR. Infrared spectroscopic studies of ammonia adsorbed on V_2O_5-MoO_3/ZrO_2 catalysts showed the presence of both Lewis and Brönsted acids.

Acknowledgment. This work was supported by Korea Research Foundation Grant (KRF-2001-041-E00312).

References

1. Argyle, M. D.; Chen, K.; Bell, A. T.; Iglesia, E. *J. Catal.* **2002**, *208*, 139.
2. Miyata, H.; Kohno, M.; Ono, T.; Ohno, T.; Hatayama, F. *J. Chem. Soc., Faraday Trans. 1* **1989**, *85*, 3663.
3. Lakshmi, L. J.; Ju, Z.; Alyea, E. *Langmuir* **1999**, *15*, 3521.
4. Bulushev, D. A.; Kiwi-Minsker, L.; Zaikovskii, V. I.; Renken, A. *J. Catal.* **2000**, *193*, 145.
5. Feng, T.; Vohs, J. M. *J. Catal.* **2002**, *208*, 301.
6. Busca, G.; Elmi, A. S.; Forzatti, P. *J. Phys. Chem.* **1987**, *91*, 5263.
7. Narayama, K. V.; Masthan, S. K.; Rao, V. V.; Raju, B. D.; Rao, P. K. *Catal. Commun.* **2002**, *3*, 173.
8. Jung, S. M.; Grange, P. *Appl. Catal. B : Environmental* **2001**, *32*, 1230.
9. Alemany, L. J.; Lietti, L.; Ferlazzo, N.; Forzatti, P.; Busca, G.; Giamello, E.; Bregani, F. *J. Catal.* **1995**, *155*, 117.
10. Centeno, M. A.; Malet, P.; Carrizosa, I.; Odriozola, J. A. *J. Phys. Chem. B* **2000**, *104*, 3310.
11. Matralis, H. M.; Ciardelli, M.; Ruwet, M.; Grange, P. *J. Catal.* **1995**, *157*, 368.
12. Elmi, A. S.; Tronoconi, E.; Cristiani, C.; Martin, J. P. G.; Forzatti, P. *Ind. Eng. Chem. Res.* **1989**, *84*, 387.
13. Lapina, O. B.; Shubin, A. A.; Nosov, A. V.; Bosch, E.; Spengler, J.; Knözinger, H. *J. Phys. Chem. B* **1999**, *103*, 7599.
14. Gao, X.; Jehng, J.-M.; Wachs, I. E. *J. Catal.* **2002**, *209*, 43.
15. Hatayama, F.; Ohno, T.; Maruoka, T.; Ono, T.; Miyata, H. *J. Chem. Soc., Faraday Trans.* **1991**, *87*, 2629.
16. Reddy, B. M.; Ganesh, I.; Reddy, E. P.; Fernandez, A.; Smirniotis, P. G. *J. Phys. Chem. B* **2001**, *105*, 6227.
17. Centi, G.; Pinelli, D.; Trifiro, F.; Ghoussoub, D.; Guelton, M.; Gengembre, L. *J. Catal.* **1991**, *130*, 238.
18. Li, M.; Shen, J. *J. Catal.* **2002**, *205*, 248.
19. Scharf, U.; Schraml-Marth, M.; Wokaun, A.; Baiker, A. *J. Chem. Soc., Faraday Trans. 1* **1991**, *87*, 3299.
20. Monaci, R.; Rombi, E.; Solinas, V.; Sorrentino, A.; Santacesania, E.; Colon, G. *Appl. Catal. A: General* **2001**, *214*, 203.
21. Sohn, J. R.; Park, M. Y.; Pae, Y. I. *Bull. Korean Chem. Soc.* **1996**, *17*, 274.
22. Sohn, J. R.; Kim, J. G.; Kown, T. D.; Park, E. H. *Langmuir* **2002**, *18*, 1666.
23. Ward, D. A.; Ko, E. I. *J. Catal.* **1994**, *150*, 18.
24. Hassan, El-B.; Mun, S. P. *J. Ind. Eng. Chem.* **2002**, *8*, 359.
25. Hsu, C. Y.; Heimbuch, C. R.; Armes, C. T.; Gates, B. C. *J. Chem. Soc. Chem. Commun.* **1992**, 1645.

26. Wan, K. T.; Khouw, C. B.; Davis, M. E. *J. Catal.* **1996**, *158*, 311.
27. Iglesia, E.; Soled, S. L.; Kramer, G. M. *J. Catal.* **1993**, *144*, 238.
28. Ebitani, K.; Konishi, J.; Hattori, H. *J. Catal.* **1991**, *130*, 257.
29. Vaudagna, S. R.; Comelli, R. A.; Canavese, S. A.; Figoli, N. S. *J. Catal.* **1997**, *169*, 389.
30. Zhao, B.; Wang, X.; Ma, H.; Tang, Y. *J. Mol. Catal. A:Chemical* **1996**, *108*, 167.
31. Larsen, G.; Lotero, E.; Parra, R. D. *in Proc. 11th Int. Congr. Catal.* **1996**, 543.
32. Kera, Y.; Hirota, K. J. *Phys. Chem.* **1969**, *73*, 3937.
33. Cole, D. J.; Cullis, C. F.; Hucknall, D. J. *J. Chem. Soc. Faraday Trans. 1* **1976**, *72*, 2185.
34. Sohn, J. R.; Cho, S. G.; Pae, Y. I.; Hayashi, S. *J. Catal.* **1996**, *159*, 170.
35. Park, E. H.; Lee, M. H.; Sohn, J. R. *Bull. Korean Chem. Soc.* **2000**, *21*, 913.
36. Sohn, J. R.; Doh, I. J.; Pae, Y. I. *Langmuir* **2002**, *18*, 6280.
37. Mori, K.; Miyamoto, A.; Murakami, Y. *J. Chem. Soc., Faraday Trans. 1* **1987**, *83*, 3303.
38. Bjorklund, R. B.; Odenbrand, C. U. I.; Brandin, J. G. M.; Anderson, L. A. H.; Liedberg, B. *J. Catal.* **1989**, *119*, 187.
39. Highfield, J. G.; Moffat, J. B. *J. Catal.* **1984**, *88*, 177.
40. Roozeboom, F.; Mittelmeijer-Hazeleger, M. C.; Moulijn, J. A.; Medema, J.; de Beer, U. H. J.; Gelling, P. J. *J. Phys. Chem.* **1980**, *84*, 2783.
41. Desikan, A. N.; Huang, L.; Oyama, S. T. *J. Phys. Chem.* **1991**, *95*, 10050.
42. Liu, Z.; Chen, Y. *J. Catal.* **1998**, *177*, 314.
43. Dines, T. J.; Rochester, C. H.; Ward, A. M. *J. Chem. Soc. Faraday Trans. 1* **1991**, *87*, 653.
44. Dufresne, P.; Payen, E.; Grimblot, J.; Bonnelle, J. P. *J. Phys. Chem.* **1981**, *85*, 2344.
45. Hu, H.; Wachs, I. E. *J. Phys. Chem.* **1995**, *99*, 10897.
46. Ramis, G.; Cristiani, C.; Forzotti, P.; Busca, G. *J. Catal.* **1990**, *124*, 574.
47. Schild, C. H.; Wokaun, A.; Köppel, R. A.; Baiker, A. *J. Catal.* **1991**, *130*, 657.
48. Scheithauer, M.; Grasselli, R. K.; Knözinger, H. *Langmuir* **1998**, *14*, 3019.
49. Eckert, H.; Wachs, I. E. *J. Phys. Chem.* **1989**, *93*, 6796.
50. Reddy, B. M.; Reddy, E. P.; Srinivas, S. T.; Mastikhim, V. M.; Nosov, N. V.; Lapina, O. B. *J. Phys. Chem.* **1992**, *96*, 7076.
51. Le Costumer, L. R.; Taouk, B.; Le Meur, M.; Payen, E.; Guelton, M.; Grimblot, J. *J. Phys. Chem.* **1998**, *92*, 1230.
52. Larsen, G.; Lotero, E.; Petkovic, L. M.; Shobe, D. S. *J. Catal.* **1997**, *169*, 67.
53. Afanasiev, P.; Geantet, C.; Breysse, M.; Coudurier, G.; Vedrine, J. C. *J. Chem. Soc., Faraday Trans. 1* **1994**, *190*, 193.
54. Larrubia, M. A.; Ramis, G.; Busca, G. *Appl. Catal. B: Environmental* **2000**, *27*, L145.
55. Satsuma, A.; Hattori, A.; Mizutani, K.; Furuta, A.; Miyamoto, A.; Hattori, T.; Murakami, Y. *J. Phys. Chem.* **1988**, *92*, 6052.